doi.org/10.36721/PJPS.2020.33.6.SUP.2847-2857.1

Dual-targeting potential of active constituents of *Nigella sativa* against FimH and CTX-M-15: A plausible therapeutic strategy against drug-resistant uropathogenic strains

Hany Ezzat Khalil[1,2]*, Sibhghatulla Shaikh[3], Syed Mohd Danish Rizvi[4], Afrasim Moin[4], Amr S Abu Lila[4], Tamer M Shehata[1] and Heba S Elsewedy[1]

[1]Department of Pharmaceutical Sciences, College of Clinical Pharmacy, King Faisal University, Al-Ahsa, Saudi Arabia
[2]Department of Pharmacognosy, Faculty of Pharmacy, Minia University, Minia, Egypt
[3]Department of Medical Biotechnology, Yeungnam University, South Korea
[4]Department of Pharmaceutics, University of Hail, Saudi Arabia

Abstract: Uropathogenic strains belonging to the *Enterobacteriaceae* family are considered one of factors for urinary tract infections, and type 1 pilus fimbrial adhesin (FimH) and beta lactamase CTX-M-15 play crucial roles in their pathogenesis and resistance. Thus, a promising approach is to explore dual-targeting therapeutic agents that act against both FimH and CTX-M-15. In the present study, active constituents of *Nigella sativa* were selected on the basis of significant activity against UTIs. Molecular docking was used to target active constituents of *Nigella sativa* to the active sites of FimH and CTX-M-15*;* these included thymoquinone, dithymoquinone, carvacrol, p-cymene, thymol, thymohydroquinone and longifolene. Dithymoquinone was found to be the most potent dual inhibitor, with binding energy of -7.01 and -5.38kcal/mol against CTX-M-15 and FimH, respectively; In addition, Dithymoquinone exhibited superior activity compared to positive controls avibactam and heptyl α-D-mannopyranoside. Further molecular dynamic simulation studies were carried out to assess the stability of dithymoquinone-target protein complexes via RMSD, Rg, SASA, hydrogen bond number, and RMSF analysis. Both protein-ligand complexes were conserved and attained equilibrium at around 2.0 to 2.5 ns during10 ns runs. These results suggest that active constituents of *Nigella sativa*, particularly dithymoquinone, might represent a plausible therapeutic strategy against resistant uropathogenic bacteria.
.

Keywords: CTX-M-15, FimH, multi-drug resistance, *Nigella sativa,* urinary tract infections.

INTRODUCTION

The most prevalent bacterial infections in clinical settings are urinary tract infections (UTIs) (Foxman, 2010). Globally, these affect nearly 150 million individuals every year and are more predominant in the female population than the male (Gonzalez and Schaeffer, 1999, Harrington and Hooton, 2000). Uropathogenic bacterial species of the *Enterobacteriaceae* family are considered the key causative organism for UTIs (Adwan *et al*., 2014, Tayh *et al*., 2019). The majority of UTIs are caused by *Escherichia coli* (accounting for 80%), followed by *Klebsiella*, *Acinetobacter*, *Enterobacter*, *Pseudomonas*, *Serratia*, and *Proteus* species and finally *Enterococcus* and *Staphylococcus* species as causative Gram-positive pathogens for the remainder of infections (Mohammed *et al*., 2016). Recently, the incidence of complicated UTIs caused by resistant gram-negative bacteria has increased, presumably due to the spread of bacteria possessing extended spectrum β-lactamases (ESBLs), which present a great therapeutic challenge (Eltai *et al*., 2018). ESBLs are a group of enzymes that hydrolyze antimicrobial agents and render them ineffective; among these, the most frequent enzymes are the CTX-M class (Cantón and Coque, 2006, Shaikh *et al*., 2016a). named for being more highly active against cefotaxime than against ceftazidime (Bauernfeind *et al*., 1992). Within the CTX-M family, type 15 (CTX-M-15) is the most prevalent in uropathogenic strains (Shakil and Khan, 2010a, Zorgani *et al*., 2017, Hussain *et al*., 2012).

Beside this, initial aspect of any UTIs is the attachment or adherence of uropathogenic strain to the host mucosal surface. Type 1 pilus fimbrial adhesin FimH located on type 1 pili of uropathogenic bacterial strains are indeed responsible for this attachment (Stahlhut *et al*., 2009, Krammer *et al*., 2018). Glycoproteins existing on the surface of urinary tract epithelial cell are the adhesive factors for these FimH (Krammer *et al*., 2018, Zhou *et al*., 2001). More generally, adherence to the host cell surface is considered fundamental for any bacterial invasion (Hung *et al*., 2002). The initial aspect of any UTI is the attachment or adherence of a uropathogenic strain to the host mucosal surface; the type 1 pilus fimbrial adhesin (FimH) is responsible for this attachment (Mydock-McGrane *et al*., 2016). Furthermore, this strategy has some additional benefits over the available antibiotics: The host's normal flora remain unaffected, targeting the adherence process has no bactericidal action and therefore less concern of resistance and the attachment mechanisms

**Corresponding author:* e-mail: heahmed@kfu.edu.sa

of particular bacterial strains can be targeted with precise specificity (Krammer *et al*., 2018).

The current study explored active constituents of *Nigella sativa* as natural dual inhibitors targeting two aspects of infection by uropathogenic bacterial strains: Attachment via FimH and resistance due to ESBLs, namely CTX-M-15. *N. sativa* and its components have been extensively explored for pharmacological potential, including antibacterial activity against different uropathogenic strains (Chaieb *et al*., 2011, Namjoo *et al*., 2013, Forouzanfar *et al*., 2014, Hayatdavoudi *et al*., 2016, Utami and Diagnosis, 2018, Dhanasekaran, 2019, Alqannam and Health, 2020, Basavegowda *et al*., 2020). Moreover, *N. sativa* extracts have shown protective effects against nephrotoxicity caused by gentamicin (Namjoo *et al*., 2013). Recently, ethanolic extracts of *N. sativa* have even been reported to modify the mechanism of multiple drug resistance in uropathogenic bacterial strains (Dhanasekaran, 2019). Based on these reports, selected compounds of *N. sativa* were used for current study. The major active components of *N. sativa* are p-cymene, carvone, trans-anethole, α-thujene, β-pinene, limonene, thymohydroquinone, carvacrol, thymoquinone, thymol, longifolene, dithymoquinone and α-pinene (Srinivasan, 2018, Ali and Blunden, 2003, Boskabadi and Shirmohammadi, 2002, Hammadi *et al*., 2020, Elariny *et al*.). Among these, several reports have documented immense antimicrobial potential for thymoquinone (Forouzanfar *et al*., 2014, Chaieb *et al*., 2011, Basavegowda *et al*., 2020); namely, thymoquinone has found to prevent biofilm formation by *Cronobacter sakazakii* 7-17 and hindered quorum sensing in *Cronobacter sakazakii* ATCC 29544 (Shi *et al*., 2017). Nonetheless, the present study explored all above-mentioned major active constituents of *N. sativa* for dual targeting potential against CTX-M-15 and FimH. Molecular docking experiments were performed to identify the best dual inhibitors, followed by a molecular dynamics simulation study of the best-docked structure to evaluate its stability. The results suggest that a dithymoquinone scaffold might be explored further to design novel inhibitors that could simultaneously overcome resistance, impede attachment and exert antibacterial potential against uropathogenic strains.

MATERIALS AND METHODS

Retrieval of compound and protein structures

The 3-dimensional structures of FimH (ID: 4AV5) and CTX-M-15 (ID: 4S2I) were fetched from the Protein Data Bank. Those for trans-anethole (Chemspider ID: 637563), p-cymene (Chemspider ID: 7463), limonene (Chemspider ID: 22311), carvone (Chemspider ID: 7439), α-thujene (Chemspider ID: 17868), thymoquinone (Chemspider ID: 10281), thymohydroquinone (Chemspider ID: 95779), dithymoquinone (Chemspider ID: 398941), carvacrol (Chemspider ID: 10364), β-pinene (Chemspider ID: 10290825), thymol (Chemspider ID: 6989), longifolene (Chemspider ID: 289151), α-pinene (Chemspider ID: 6654), avibactam (Chemspider ID: 9835049), and heptyl α-D-mannopyranoside (Chemspider ID: 11300413) were retrieved from the PubChem database.

Molecular docking

The compounds were docked to FimH and CTX-M-15 using 'Autodock4.2' (Scripps Research Institute, La Jolla, CA, USA). Energy of ligands was minimized using the MMFF94 force field. Kollman charges, solvation constraints and hydrogen atoms were added. To explicitly focus on the active site of CTX-M-15 and FimH, grid maps were set via Autogrid establishing 60×60×60 Å grid points with 0.375 Å spacing. For CTX-M-15, the x, y and z co-ordinates were kept as 6.930, 14.060 and 9.920, respectively to target's active site of CTX-M-15'. The docking procedure was carried out by using Solis & Wets local search and the Lamarckian genetic algorithm. For every docking test, a hundred runs were used ending upon reaching a limit of 2,500,000 energy assessments.

LIGPLOT$^+$ analysis

After performing the docking, the best ligand-CTX-M-15 and ligand-FimH complexes were analyzed by LIGPLOT$^+$ version v.2.1 (EMBL-EBI, Cambridgeshire, UK). LIGPLOT analysis assists in identifying the hydrogen-based and hydrophobic interactions between a ligand and important amino acid residues in the protein. The 3D structures so produced were transformed into 2D figs. using the LIGPLOT algorithm.

Molecular dynamic (MD) simulation study

GROMACS 5.1.5 platform (Hess *et al*., 2008) with total atom force field CHARMM27 (Bjelkmar *et al*., 2010) was used to execute molecular dynamics simulation study on the native form of CTX-M-15 and FimH both in innate and in docked complex with dithymoquinone. Swiss Param server (Zoete *et al*., 2011) with CHARMM force field was applied to generate ligand topology files, with a 1.0 nm cut-off distance to evaluate Van der Waal interactions. The Partial Mesh Ewald (PME) method was used to ascertain long-range electrostatics with a 1.0 nm cut-off for columbic interaction, with counter ions included to maintain the condition of system electro-neutrality. A TIP3P water model was used to solvate the system and protein atoms were separated from the box dimension wall by 1.0 nm to 1.5 nm during simulation in order to retain the periodic boundary conditions (Mark and Nilsson, 2001).The steepest descent algorithm with 1000 KJ/mol/nm tolerance was used for initial energy minimization of the structures. Position restrains were applied on the complex and during simulation for the equilibration of the system via NPT ensembles after canonical NVT ensembles. Each equilibration was under conditions of 300 K temperature and 1 bar pressure for a

run of 200 ps. Velocity rescaling with 0.1 ps coupling constant was used for temperature coupling and Maxwell distribution was used for the generation of initial velocities, the Parrinello-Rahman algorithm with 2ps constant coupling was used for temperature-pressure coupling. A Production run of 10 ns was performed after equilibration with a 2 fs time step integration and trajectories were saved every 500 steps (Mandal *et al*., 2018). GROMACS along with XMGRACE-5.1.22 platform were used for the final analysis.

RESULTS

Binding energy and inhibition constant values of compounds with CTX-M-15 and FimH are represented in table 1. Fig. 1 represents the molecular docking simulation, showing the interaction of β-pinene, carvone, dithymoquinone, longifolene, thymoquinone and avibactam with amino acid residues of CTX-M-15. Fig. 2 represents the molecular docking simulation, showing the interaction of β-pinene, carvone, dithymoquinone, longifolene, thymoquinone and avibactam with amino acid residues of FimH. Fig. 3 and 4 show the molecular dynamic simulation studies that performed on the best-docked structures 'CTX-M-15-dithymoquinone and 'FimH-dithymoquinone' complex, respectively to determine the dynamic behavior with respect to time under solvated environment.

DISCUSSION

E. coli is the main uropathogen (80% of UTIs), followed by *Staphylococcus saprophyticus* (10-15%), then *Klebsiella*, *Enterobacter* and *Proteus* species and finally *Enterococcus* as being uncommonly responsible for uncomplicated cystitis and pyelonephritis (Ronald, 2003). The present study investigated the dual inhibition potential of the active components of *N. sativa* against the FimH adhesion protein and ESBLs (CTX-M 15) as a strategy for overcoming UTIs caused by antibiotic-resistant bacterial pathogens.

CTX type M variants, especially blaCTX-M-15, are the most common type of ESBL (Shaikh *et al*., 2016a, Fam *et al*., 2011). The present study explored the interaction of main catalytic domain residues of CTX-M-15 with *N. sativa* extract components and found that Ser70, Lys73, Asn104, Tyr105, Tyr129, Ser130, Asn132, Glu166, Asn170, Thr216, Ser220, Lys234, Thr235, Ser237 and Arg276 were involved in interaction with *β*-pinene, carvone, dithymoquinone, longifolene and thymoquinone (Supplementary fig. S1a-S1e). Interestingly, amino acids Asn104, As132, Thr235 and Ser237 have been revealed as active site residues (Shakil and Khan, 2010c) and Glu166 has also been observed to make important contact with cefotaxime (Shakil and Khan, 2010b). In this study, Glu166 also contributed in the binding of CTX-M-15 with dithymoquinone. The free energy of binding (ΔG) and inhibition constant (Ki) values for the interactions of CTX-M-15-*β*-pinene, CTX-M-15-carvone, CTX-M-15-dithymoquinone, CTX-M-15-longifolene and CTX-M-15-thymoquinone were respectively determined to be -5.11 kcal/mol and 973.42μM, -4.63 kcal/mol and 406.43μM, -7.01kcal/mol and 7.33μM, -5.24 kcal/mol and 148.89 μM, and -5.57kcal/mol and 338.50 μM (Table 1).

The CTX-M-15 amino acid residues Ser70, Ser130, and Ser237 were found to be involved in hydrogen bonds with carvone, thymoquinone and dithymoquinone (fig. 1b, 1c and 1e). In addition, Thr216, Thr235, Gly236, and Ser237 were involved in common hydrophobic interactions with *β*-pinene, carvone, dithymoquinone, longifolene, and thymoquinone (fig. 1a-1e). Both hydrogen bonds and hydrophobic interactions have been reported to play vital roles in the binding of a ligand to its target protein (Shaikh *et al*., 2014, Shaikh *et al*., 2016b, Rizvi *et al*., 2014a). This study used avibactam as the positive control for CTX-M-15 binding and identified the amino acids Ser70, Lys73, Asn104, Tyr105, Ser130, Asn132, Thr216, Ser220, Lys234, Thr235 and Arg276 as being involved in the interaction with avibactam (Supplementary fig. S1f). These same amino acids were also involved in interactions with *β*-pinene, carvone, dithymoquinone, longifolene and thymoquinone.

Beta-lactam antibiotics bind to the catalytic site of a beta-lactamase enzyme and undergo acylation, resulting in breaking of the beta-lactam ring and formation of a transient imine intermediate. The imine intermediate may then rearrange to form an enamine intermediate with either *cis*- or *trans*- conformation. Beta-lactam inhibitors undergo the same process, but form *trans*-enamine intermediates that stabilize in the enzyme's active site, leading to inactivation of the enzyme (Drawz and Bonomo, 2010). When CTX-M-15 comes in contact with beta-lactam antibiotics, the deacylation rate is enhanced several-fold, resulting in rapid CTX-M-15 regeneration. Conversely, CTX-M-15 inhibitors reduce the enzyme's deacylation or regeneration ability by forming a stable acyl-CTX-M-15 complex. Therefore, acylation and deacylation rates determine the competence of CTX-M-15 inhibitors (Faheem *et al*., 2013). The avibactam structural class of β-lactamase (CTX-M-15) inhibitor does not contain a β-lactam core but maintains the capacity to covalently acylate targets of β-lactamase (Ehmann *et al*., 2012, Lahiri *et al*., 2014). In fact, avibactam shows a distinctive carbamyl-linkage to the catalytic serine residue of CTX-M-15 that does not decompose by the hydrolytic mechanism, as happens in the case of β-lactam-based inhibitors (Ehmann *et al*., 2012, King *et al*., 2015). The conserved Ser130 amino acid residue of CTX-M-15 plays a crucial role during the carbamylation and decarbamylation of avibactam via acting as a general acid and base, respectively.

Table 1: Binding energy and inhibition constant values of compounds with CTX-M-15 and FimH.

Compounds	CTX-M-15		FimH	
	Binding Energy (kcal/mol)	Inhibition Constant (μM)	Binding Energy (kcal/mol)	Inhibition Constant (μM)
Avibactam*	-6.27	25.51	-	-
trans-anethole	-4.04	1090	-4.38	620.75
α-pinene	-4.06	1060	-4.38	620.06
β-pinene	-5.11	973.42	-5.35	548.42
Carvacrol	-4.40	594.71	-4.24	785.38
Carvone	-4.63	406.43	-5.01	211.34
p-cymene	-3.87	1450	-4.05	1080
Dithymoquinone	-7.01	7.33	-5.38	114.78
Limonene	-4.11	975.68	-4.12	955.76
Longifoline	-5.24	148.89	-5.61	76.64
α-thujene	-3.74	1820	-3.97	1220
Thymohydroquinone	-4.19	854.38	-4.19	849.32
Thymol	-4.32	686.86	-4.25	766.69
Thymoquinone	-5.57	338.50	-5.42	106.85
Heptylα-D-mannopyranoside**	-	-	-4.72	349.56

*Positive control for CTX-M-15, **Positive control for FimH

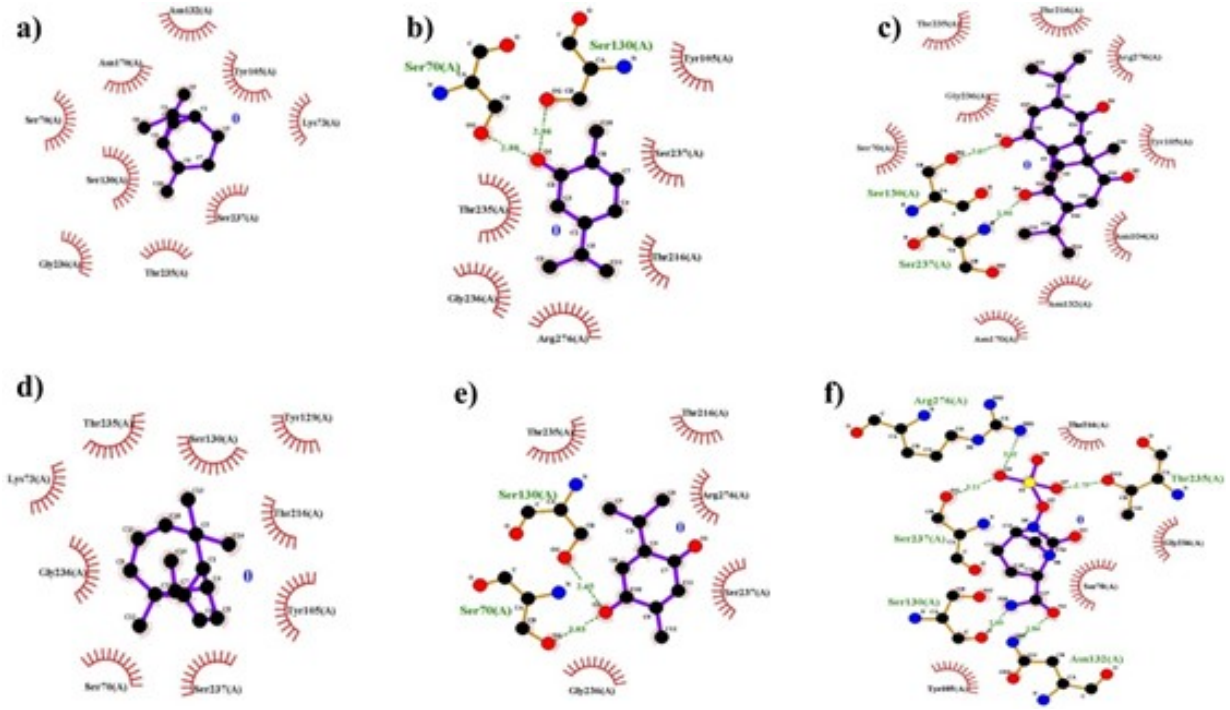

Fig. 1: Ligplot analysis of a)*β*-pinene, b)carvone, c)dithymoquinone, d)longifoline, e)thymoquinone and f)avibactam with CTX-M-15 showing the hydrophobic interacting amino acid residues (red arcs) and hydrogen bond (green dashed line).

In the carbamylation reaction, the N6 nitrogen of avibactam gets protonated after opening of the ring, and the γ-OH of Ser130 is expected to be involved in this protonation reaction. Meanwhile, Lys73 and Lys234 play important roles in the activation of Ser130 during recyclization/ decarbamylation (King *et al*., 2015). In addition, Ser70 is also considered as a key interacting residue of CTX-M-15 in the acylation of an inhibitor (King *et al*., 2015, Lahiri *et al*., 2013, Winkler *et al*., 2015). Interestingly, in this study, all of these amino acids and especially the Ser70 and Ser130 residues were found to be common interacting residues of *β*-pinene, carvone, dithymoquinone, longifolene and thymoquinone (fig. 1a-1e).

FimH adhesion promotes colonization of uropathogenic bacteria on the host cell surface, resulting in biofilm formation (Anderson *et al.,* 2003). hence, this

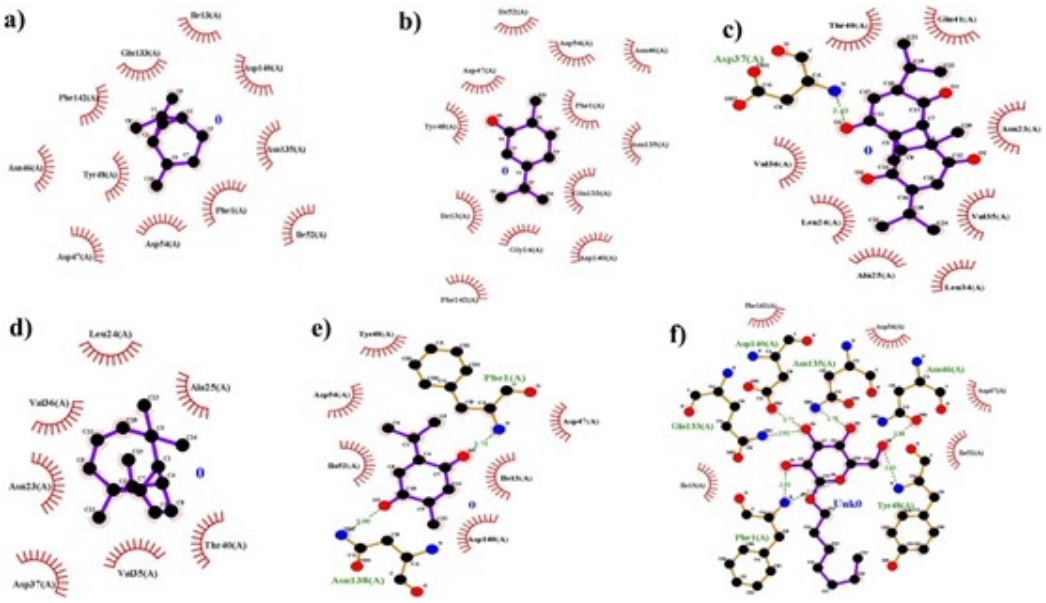

Fig. 2: Ligplot analysis of a) *β*-pinene, b) carvone, c) dithymoquinone, d) longifoline, e) thymoquinone and f) heptyl-α-D-mannopyranoside with FimH showing the hydrophobic interacting amino acid residues (red arcs) and hydrogen bond (green dashed line).

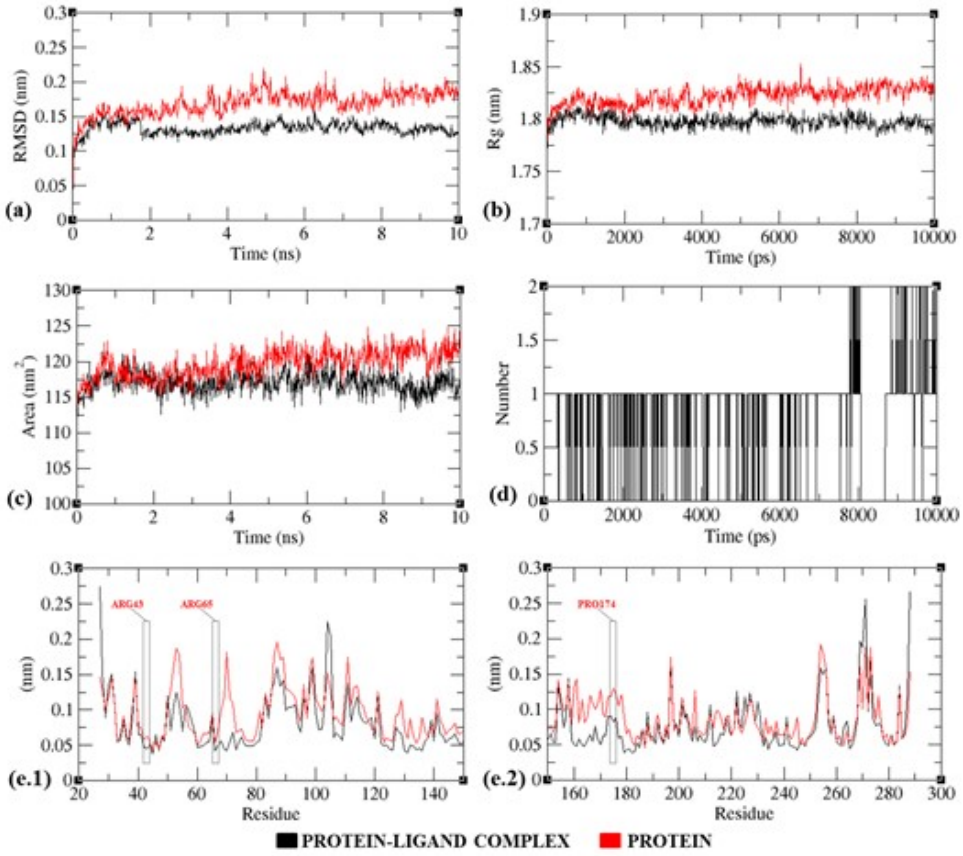

Fig. 3: RMSD, *Rg*, SASA, hydrogen bonds and RMSF exploration of complex 'CTX-M-15 with dithymoquinone' at 10000 ps. (a) RMSD time evolution for CTX-M-15 alone and with dithymoquinone complex. (b) Protein backbone *Rg* analysis for CTX-M-15 alone and with dithymoquinone complex during the total simulation time. Here, time interval (ps) is abscissa and *Rg* (nm) is ordinate. (c) SASA is indicated, where time interval (ps) is abscissa and SASA (nm) is ordinate. (d) Hydrogen bonds forming between CTX-M-15 and dithymoquinone during the total simulation time. (e.1 and e.2) Average RMSF analysis of CTX-M-15 and dithymoquinone residue wise.

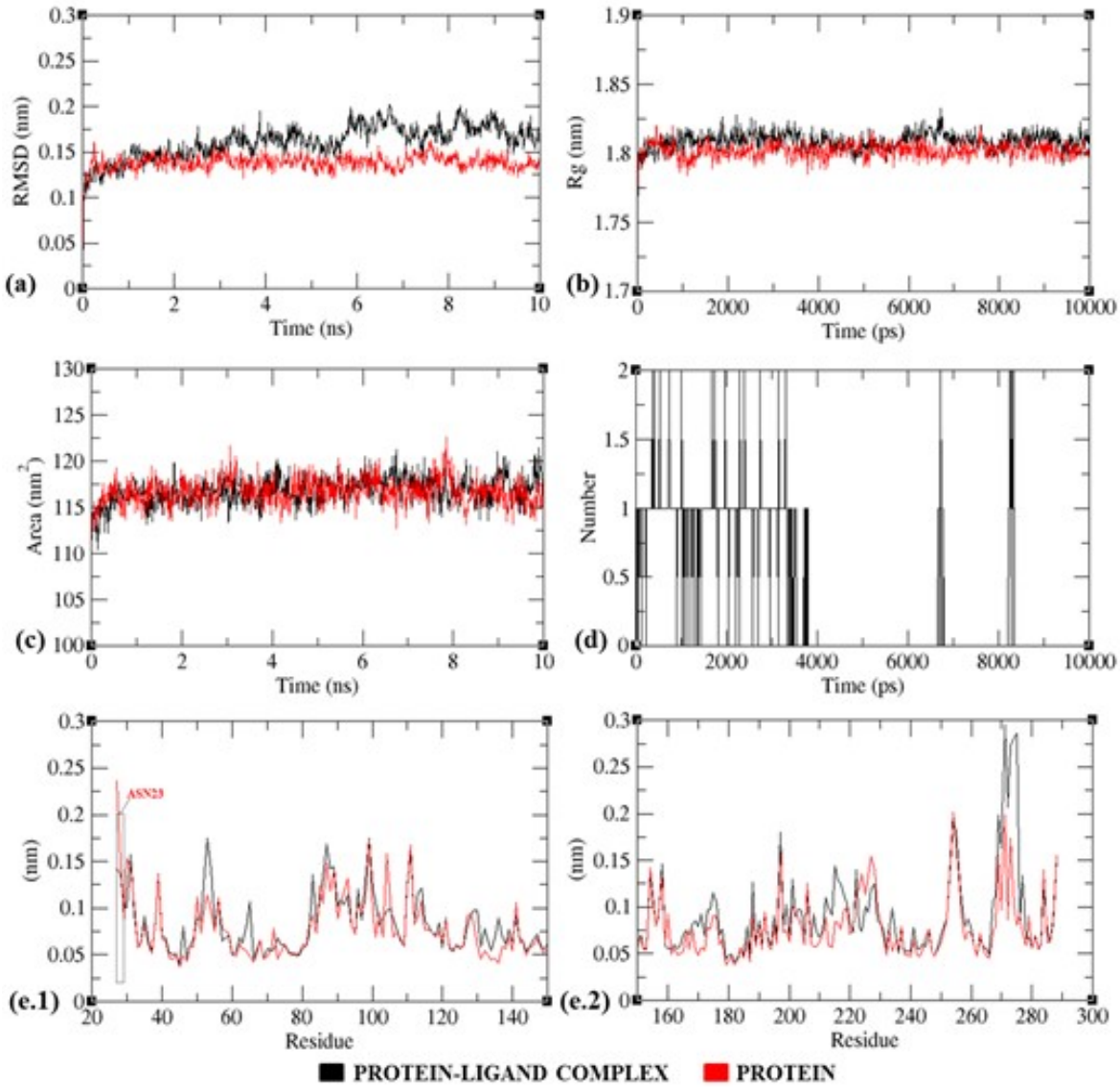

Fig. 4: RMSD, *Rg*, SASA, hydrogen bonds and RMSF exploration of complex 'FimH with dithymoquinone' at 10000 ps. (a) RMSD time evolution for FimH alone and with dithymoquinone complex. (b) Protein backbone *Rg* analysis for FimH alone and with dithymoquinone complex during the total simulation time. Here, time interval (ps) is abscissa and *Rg* (nm) is ordinate. (c) SASA is indicated, where time interval (ps) is abscissa and SASA (nm) is ordinate. (d) Hydrogen bonds forming between FimH and dithymoquinone during the total simulation time. (e.1 and e.2) Average RMSF analysis of FimH and dithymoquinone residue wise.

adhesion protein has been regarded as a potential therapeutic target for treating UTIs (Mydock-McGrane *et al*., 2016). In terms of interactions with tested compounds, this study found the FimH functional domain to interact with *β*-pinene through 11 amino acids, specifically Phe1, Ile13, Asn46, Asp47, Tyr48, Ile52, Asp54, Gln133, Asn135, Asp140 and Phe142 (Supplementary fig. S2a); with carvone through 12 amino acids, namely Phe1, Ile13, Gly14, Asn46, Asp47, Tyr48, Ile52, Asp54, Gln133, Asn135, Asp140 and Phe142 (Supplementary fig. S2b); with dithymoquinone via eight amino acids, namely Val22, Asn23, Leu24, Ala25, Leu34, Val35, Asp37 and Thr40 (Supplementary fig. S2c); with longifolene via eight amino acids, namely Val22, Asn23, Leu24, Ala25, Val35, Val36, Asp37 and Thr40 (Supplementary fig. S2d); and with thymoquinone through ten amino acids, namely Phe1, Ile13, Asp47, Tyr48, Ile52, Asp54, Gln133, Asn136, Asn138 and Asp140 (Supplementary fig. S2e).

The ΔG and Ki values for the interactions of FimH-*β*-pinene, FimH-carvone, FimH-dithymoquinone, FimH-longifoline and FimH-thymoquinone were determined to be -5.35 kcal/mol and 548.42μM, -5.01kcal/mol and 211.34μM, -5.38 kcal/mol and 114.78μM, -5.61kcal/mol

and 76.64µM and -5.42kcal/mol and 106.85µM, respectively (table 1). The FimH amino acid residues Phe1, Ile13, Gly14, Asn46, Asp47, Tyr48, Pro49, Thr51, Ile52, Asp54, Thr134, Asn135, Asp140, Phe142 were found to be involved in interaction with its antagonist heptyl α-D-mannopyranoside (Supplementary fig. S2f). Notably, the key FimH binding pocket residues are Phe1, Asn46, Asp47, Asp54, Glu133, Asn135, Asp140 and Phe142; mutation in any of these residues affects FimH function and also decreases virulence (Hung *et al*., 2002, Chen *et al*., 2009). This study found these FimH amino acids to also be involved in binding with active components of *N. sativa* (*β*-pinene, carvone, dithymoquinone, longifolene, and thymoquinone).

The FimH adhesin has two domains, the C-terminal pilin domain that anchors it to the pilus rod and the N-terminal lectin domain. Adherence of the uropathogen *E. coli* is promoted by binding of the FimH lectin domain to specific mannose-containing molecules on the epithelial cell surface (Snyder *et al*., 2006). The FimH lectin domain has a mannose-binding pocket (Asn46, Asp47, Asp54, Gln133, Asn135, Asn138 and Asp140) that interacts with the sugar via various hydrogen bonds. Hydrophobic regions are present in the structural surround of the mannose-binding pocket and consist of hydrophobic support (Phe1, Ile13 and Phe142), the 'tyrosine gate' (Tyr48, Ile52 and Tyr137) and the residue Thr51 (Mydock-McGrane *et al*., 2016). Interestingly, in this study, FimH amino acids Phe1, Ile13, Asn46, Asp47, Tyr48, Ile52, Asp54, Gln133, Asn135, Asp140 and Phe142 contributed to its interaction with *β*-pinene, carvone and thymoquinone (fig. 2a, 2b and 2e).

Mannose is a probable inhibitor of the attachment of *E. coli* to epithelial cells of the human intestine; this was first reported way back in 1957 (Duguid *et al*., 1957), but continued to be ignored until the pivotal work of Nathan Sharon in 1977 (Ofek *et al*., 1977) which reported concrete information on the mannose-mediated attachment of *E. coli* K12 and B strains to intestinal epithelial cells. An interesting finding of that study was discovery of a 'lectin-like' material on the *E. coli* surface, which was later named FimH. Through competitive inhibition assays, it was observed that α-D-mannose and methyl α-D-mannopyranoside (αMM) have the potential to avert binding of *E. coli* to human epithelial cells, and furthermore to displace already-attached *E. coli* from the epithelial cells. Two years later, Aronson *et al*. emphasized the potential role of αMM in preventing *E. coli* colonization in the urinary tract of mice via blocking bacterial adherence (Aronson *et al*., 1979). With these proof-of-concept studies, the FimH lectin was recognized as a potential target for UTI therapy. Later on, several reports suggested the applicability of different FimH antagonists specifically against uropathogens (Mydock-McGrane *et al*., 2016, Sarshar *et al*., 2020, Mydock-McGrane *et al*., 2017). and aryl and hydrophobic substitution of α-D-mannose significantly increased its potency as a FimH (*E. coli*) antagonist (Mousavifar *et al*., 2019). In fact, relative inhibitory antagonist potential is defined by the hydrophobicity and conformity of aglycone moieties and their orientation on the primary carbohydrate molecule (Ribić *et al*., 2018, Hartmann and Lindhorst, 2011). In particular, substitution with biphenyl derivatives could confer additional advantages on a FimH antagonist. It has been observed that the addition of 1,10-biphenyl pharmacophore along with different aglycone atoms to α-D-mannose derivatives increased their suitability as FimH antagonists (Mousavifar *et al*., 2019, Mousavifar *et al*., 2018). These modifications would increase oral/intestinal absorption and the metabolic stability of modified mannosides and further promote efficient reabsorption via kidney tubuli, leading to increased dosage at the infection site via frequent excretion in urine (Mayer *et al*., 2017, Klein *et al*., 2010, Schwardt *et al*., 2011). In addition, mannose scaffold-based glycomimetics have also been synthesized and extensively explored for their ability as FimH antagonists (Sarshar *et al*., 2020, Ribić *et al*., 2018). Beyond these synthetic compounds, natural compounds like proanthocyanidins, proanthocyanidin-derived metabolites of polyphenols and myricetin have shown strong anti-adhesive properties against uropathogenic *E. coli* (Rafsanjany *et al*., 2015).

Natural α-D-mannosides from herbal sources have already been explored in several trials as supplements or for use in addition to antibiotics for UTI treatment and prevention (Domenici *et al*., 2016, Genovese *et al*., 2018). In 2016, Enterome procured a license from Vertex for a FimH mannoside portfolio and presented EB8018 as a FimH antagonist. According to the opinion of Mydock-McGrane *et al*. EB8018 is expected to be a divalent mannoside. Moreover, it entered a phase 1 trial in early 2017 for treatment of Crohn's Disease. Simultaneously, several monovalent mannosides (O- and C-) have been developed for treatment of UTI patients with better efficacy, stability and bioavailability. In addition, Fimbrion Therapeutics also collaborated with GlaxoSmithKline at the end of 2016 for the preclinical evaluation of oral mannosides to transform them into a novel therapy against UTIs (Mydock-McGrane *et al*., 2017).

This study used docking analysis and molecular dynamic simulation studies to evaluate natural compounds in *N. sativa* extract for potential use in UTI treatment. In docking analysis, ΔG determines the strength of interaction between ligand and target protein, with higher (negative) binding energy indicating efficient binding (Verma *et al*., 2014, Rizvi *et al*., 2014b). Compared with the positive control heptyl α-D-mannopyranoside, the obtained binding energy values revealed strong

interactions with FimH for *β*-pinene, carvone, dithymoquinone, longifolene and thymoquinone. Meanwhile, relative to the interaction of avibactam with CTX-M-15, similar binding energies were observed for *β*-pinene, carvone, longifolene and thymoquinone, while dithymoquinone exhibited more efficient interaction than avibactam in terms of binding energy.

Molecular dynamic simulation studies were performed on the best-docked structures, i.e. CTX-M-15-dithymoquinone and FimH-dithymoquinone, to determine their dynamic behavior and stability with respect to time under a solvated environment, providing further insight into binding ability. The values analyzed were root mean square deviation (RMSD), radius of gyration (R_g), solvent accessible surface area (SASA), number of hydrogen bonds, root mean square fluctuation (RMSF), and secondary structure pattern variation amongst the native protein and complex. Four different simulations of 10 ns duration were executed with the protein alone and with the ligand-protein complex.

The RMSD plot showed that all protein-ligand complexes attained equilibrium at around 2.0-2.5 ns and maintained it from there on (fig. 3a and 4a), showing a stable trajectory with slight deviation in the range of 0.10-0.15 nm RMSD. These results indicate that the structural flexibility of these proteins was conserved in the ligand-bound complex form rather than the unbound free form. Interestingly, the unbound free proteins reached equilibrium after an initial fluctuation, while ligand-bound proteins attained stable trajectories much faster in comparison. R_g considers the root mean square distances of masses in a molecule relative to its central rotation axis. More specifically, the R_g plot depicts the capability, folding, and shape of the protein through every time step of the entire trajectory during the simulation (fig. 3b and 4b). Both native proteins and their ligand-bound forms showed similar R_g value patterns throughout the simulation, with a deviation range of 1.8-1.85nm. The zones around the hydrophobic cores of protein-ligand complexes were further evaluated by SASA (fig. 3c and 4c), yielding steady SASA values with a typical fluctuation range of 115-120nm^2. Hydrogen bonds observed in the docking study were analyzed over the total period of the simulation study, with only intermolecular H-bonds between ligands and protein being taken into consideration (fig. 3d and 4d). Subsequent plots showed that H-bond numbers fluctuated with time. In case of FimH, the overall disappearance of H-bonds suggested drug release from the binding cavity because of concurrent breaking and re-building of bonds. The RMSF plot likewise showed apparent residue-wise fluctuations (fig. 3e.1, 3e.2, 4e.1 and 4.e.2). Here, significant amino acids involved in interaction were rigidified in the complex form, in contrast to their state in the native protein. It is worth to mention that *in silico* outcomes usually correlate well with wet-lab results (Rizvi *et al*., 2016, Begum *et al*., 2018, Castro *et al*., 2019, Malik *et al*., 2019, Oraiopoulou *et al*., 2018, Kim *et al*., 2013). Altogether, this study suggests that dithymoquinone could be a promising dual inhibitor against CTX-M-15 and FimH for use in the treatment of antimicrobial-resistant uropathogens responsible for UTIs. However, further microbiological and *in vivo* studies are urged to provide proof of our concept.

CONCLUSION

In the present study, the major active constituents of *N. sativa* were screened for their antibacterial potential against antibiotic resistance and attachment mechanisms via simultaneously targeting CTX-M-15 and FimH. Interestingly, molecular docking analysis revealed dithymoquinone as having promise against both these targets, including demonstrated stability when in complex form with each target protein. These results suggest that a dithymoquinone scaffold might be investigated further to design multi-targeting inhibitors against uropathogenic strains that could inhibit adherence, overcome resistance issues, and simultaneously possess bactericidal potential.

ACKNOWLEDGMENTS

The authors extend their appreciation to the Deputyship for Research & Innovation, Ministry of Education in Saudi Arabia for funding this research work through the project number (IFT20089).

REFERENCES

Adwan K, Jarrar, N, Abu-Hijleh A, Adwan G and Awwad E (2014). Molecular characterization of *Escherichia coli* isolates from patients with urinary tract infections in Palestine. *J. Medical Microbiol*., **63**(2): 229-234.

Ali BH and Blunden G (2003). Pharmacological and toxicological properties of *Nigella sativa*. *Phytother. Res.,* **17**(4): 299-305.

Alqannam R (2020). Antibacterial and Alteration of drug resistance activities of black cumin seed (*Nigella Sativa*) extracts against urinary pathogens. *J. Infect. Public Health,* **13**(2): 321-322.

Anderson GG, Palermo JJ, Schilling JD, Roth R, Heuser J and Hultgren SJ (2003). Intracellular bacterial biofilm-like pods in urinary tract infections. *Science*, **301**(5629): 105-107.

Aronson M, Medalia O, Schori L, Mirelman D, Sharon N and Ofek I (1979). Prevention of colonization of the urinary tract of mice with *Escherichia coli* by blocking of bacterial adherence with methyl alpha-D-mannopyranoside. *J. Infect. Dis.,* **139**(3): 329-32.

Basavegowda N, Patra JK and Baek KH (2020). Essential oils and mono/bi/tri-metallic nanocomposites as alternative sources of antimicrobial agents to combat

multidrug-resistant pathogenic microorganisms: an overview. *Molecules*, **25**(5): 1058.

Bauernfeind A, Holley M, Jungwirth R, Mangold P, Röhnisch T, Schweighart S, Wilhelm R, Casellas JM and Goldberg M (1992). A new plasmidic cefotaximase from patients infected with *Salmonella typhimurium*. *Infection,* **20**(3): 158-163.

Begum S, Nizami SS, Mahmood U, Masood S, Iftikhar S and Saied S (2018). *In-vitro* evaluation and in-silico studies applied on newly synthesized amide derivatives of N-phthaloylglycine as butyrylcholinesterase (BChE) inhibitors. *Comput. Biol. Chem.,* **74**: 212-217.

Bjelkmar P, Larsson P, Cuendet MA, Hess B and Lindahl E (2010). Implementation of the CHARMM Force Field in GROMACS: Analysis of protein stability effects from correction maps, virtual interaction sites, and water models. *J. Chem. Theory Comput.,* **6**(2): 459-466.

Boskabadi M and Shirmohammadi B (2002). Effect of *Nigella sativa* on isolated guinea pig trachea. *Archives Iranian Medicine*, **5**:103-107.

Cantón R and Coque TM (2006). The CTX-M beta-lactamase pandemic. *Curr. Opin. Microbiol.,* **9**(5): 466-75.

Castro RI, Valenzuela-Riffo F and Morales-Quintana L (2019). In silico and *in vitro* analysis of the 4, 4′, 4″-((1, 3, 5-triazine-2, 4, 6-triyl) tris (azanediyl)) triphenol), an antioxidant agent with a possible anti-inflammatory function. *Biomed. Res. Int.*, doi: 10.1155/2019/9165648.

Chaieb K, Kouidh B, Jrah H, Mahdouani K and Bakhrouf A (2011). Antibacterial activity of thymoquinone, an active principle of *Nigella sativa* and its potency to prevent bacterial biofilm formation. *BMC Complement. Altern. Med.*, **11**(1): 29.

Chen SL, Hung CS, Pinkner JS, Walker JN, Cusumano CK, Li Z, Bouckaert J, Gordon JI and Hultgren SJ (2009). Positive selection identifies an *in vivo* role for FimH during urinary tract infection in addition to mannose binding. *Proc. Natl. Acad. Sci.,* **106**(52): 22439-22444.

Dhanasekaran S (2019). Research article alteration of multi-drug resistance activities by ethanolic extracts of *Nigella sativa* against urinary pathogens. *Int. J. Pharmacol.,* **15**: 962-969.

Domenici L, Monti M, Bracchi C, Giorgini M, Colagiovanni V, Muzii L and Benedetti panici P. (2016). D-mannose: A promising support for acute urinary tract infections in women. A pilot study. *Eur. Rev. Med. Pharmacol. Sci.,* **20**(13): 2920-2925.

Drawz SM and Bonomo R A (2010). Three decades of beta-lactamase inhibitors. *Clin. Microbiol. Rev.,* **23**(1): 160-201.

Duguid JP and Gillies RR (1957). Fimbrias and Adhesive Properties in Dysentery Bacilli. *J. Pathol. Bacteriol.,* **74**(2): 397-411.

Ehmann DE, Jahić H, Ross PL, Gu R, Hu J, Kern G, Walkup GK and Fisher SL (2012). Avibactam is a co-valent, reversible, non-β-lactam β-lactamase inhibitor. *Proc. Natl. Acad. Sci.,* **109**(29): 11663-11668.

El-ariny E, Amer A, El-senosy Y and Naaom S (2020). Antimicrobial activity of *Nigella Sativa* and *Lawsonia inermis* (Henna) against Gram negative bacteria isolated from clinical samples. *j. biotechnol. biochem*, **6**(3): 32-37.

Eltai NO, Al Thani AA, Al-Ansari K, Deshmukh AS, Wehedy E, Al-Hadidi SH and Yassine HM (2018). Molecular characterization of extended spectrum β -lactamases enterobacteriaceae causing lower urinary tract infection among pediatric population. *Antimicrob. resist. in.,* **7**(1): 90.

Faheem M, Rehman MT, Danishuddin M and Khan AU (2013). Biochemical characterization of CTX-M-15 from *Enterobacter cloacae* and designing a novel non-β-lactam-β-lactamase inhibitor. *PLoS One,* **8**(2): e56926.

Fam N, Leflon-Guibout V, Fouad S, Aboul-Fadl L, Marcon E, Desouky D, El-Defrawy I, Abou-Aitta A, Klena J and Nicolas-Chanoine MH (2011). CTX-M-15-producing *Escherichia coli* clinical isolates in Cairo (Egypt), including isolates of clonal complex ST10 and clones ST131, ST73 and ST405 in both community and hospital settings. *Microb. Drug. Resist.,* **17**(1): 67-73.

Forouzanfar F, Bazzaz BSF and Hosseinzadeh H (2014). Black cumin (*Nigella sativa*) and its constituent (thymoquinone): a review on antimicrobial effects. *Iran J. Basic Med. Sci.* **17**(12): 929-938.

Foxman B (2010). The epidemiology of urinary tract infection. *Nat. Rev. Urol.,* **7**(12): 653-660.

Genovese C, Davinelli S, Mangano K, Tempera G, Nicolosi D, Corsello S, Vergalito F, Tartaglia E, Scapagnini G and Di Marco R (2018). Effects of a new combination of plant extracts plus d-mannose for the management of uncomplicated recurrent urinary tract infections. *J. Chemother.,* **30**(2): 107-114.

Gonzalez CM and SChaeffer AJ (1999). Treatment of urinary tract infection: what's old, what's new, and what works. *World J. Urol.,* **17**(6): 372-82.

Hammadi A, Abed H and Rabie ZH (2020). Effect extraction of nigella sativa and malricaia chamoilla on urinary tract infection. *Sci. J. Med. Res.*, **4**(16): 118-124.

Harrington RD and Hooton TM (2000). Urinary tract infection risk factors and gender. *J. Gend. Specif. Med.,* **3**(8): 27-34.

Hartmann M and Lindhorst TK (2011). The bacterial lectin FimH, a target for drug discovery-carbohydrate inhibitors of type 1 fimbriae-mediated bacterial adhesion. *European J. Org. Chem.*, **20-21**: 3583-3609.

Hayatdavoud P, Rad AK, Rajaei Z and Hadjzadeh MAR (2016). Renal injury, nephrolithiasis and *Nigella sativa*: A mini review. *Avicenna J. Phytomed.,* **6**(1): 1-8.

Hess B, Kutzner C, Van Der Spoel D and Lindahl E (2008). GROMACS 4: Algorithms for highly efficient, load-balanced, and scalable molecular simulation. *J. Chem. Theory. Comput.,* **4**(3): 435-447.

Hung CS, Bouckaert J, Hung D, Pinkner J, Widberg C, DeFusco A, Auguste CG, Strouse R, Langermann S, Waksman G and Hultgren SJ (2002). Structural basis of tropism of *Escherichia coli* to the bladder during urinary tract infection. *Mol. Microbiol.,* **44**(4): 903-15.

Hussain A, Ewers C, Nandanwar N, Guenther S, Jadhav S, Wieler LH and Ahmed N (2012). Multiresistant uropathogenic *Escherichia coli* from a region in India where urinary tract infections are endemic: Genotypic and phenotypic characteristics of sequence type 131 isolates of the CTX-M-15 extended-spectrum-β-lactamase-producing lineage. *Antimicrob. Agents Chemother.,* **56**(12): 6358-65.

Kim T, Afonin KA, Viard M, Koyfman AY, Sparks S, Heldman E, Grinberg S, Linder C, Blumenthal RP and Shapiro BA (2013). *In silico, in vitro* and *in vivo* studies indicate the potential use of bolaamphiphiles for therapeutic siRNas delivery. *Molecular Therapy-Nucleic acids,* **2**: e80.

King DT, King AM, Lal SM, Wright GD and Strynadka NC (2015). Molecular mechanism of avibactam-mediated β-lactamase inhibition. *ACS Infectious Diseases,* **1**(4): 175-184.

Klein T, Abgottspon D, Wittwer M, Rabbani S, Herold J, Jiang X, Kleeb S, Lüthi C, Scharenberg M, Bezençon J and Gubler E (2010). FimH antagonists for the oral treatment of urinary tract infections: From design and synthesis to *in vitro* and *in vivo* evaluation. *J. Med. Chem.,* **53**(24): 8627-8641.

Krammer EM, De Ruyck J, Roos G, Bouckaert J and Lensink MF (2018). Targeting dynamical binding processes in the design of non-antibiotic anti-adhesives by molecular simulation-the example of FimH. *Molecules*, **23**(7): 1641.

Lahiri SD, Johnstone MR, Ross PL, McLaughlin RE, Olivier NB and Alm RA (2014). Avibactam and class C β-lactamases: Mechanism of inhibition, conservation of the binding pocket, and implications for resistance. *Antimicrob. Agents Chemother.,* **58**(1): 5704-13.

Lahiri SD, Mangani S, Durand-Reville T, Benvenuti M, De Luca F, Sanyal G and Docquier JD (2013). Structural insight into potent broad-spectrum inhibition with reversible recyclization mechanism: Avibactam in complex with CTX-M-15 and *Pseudomonas aeruginosa* AmpC β-lactamases. *Antimicrob. Agents Chemother.,* **57**(6): 2496-2505.

Malik A, Jamil U, Butt TT, Waquar S, Gan SH, Shafique H and Jafar TH (2019). In silico and in vitro studies of lupeol and iso-orientin as potential antidiabetic agents in a rat model. *Drug Des. Devel. Ther.,* **13**: 1501-1513.

Mandal SP, Garg A, Prabitha P, Wadhwani AD, Adhikary L and Kuma BP (2018). Novel glitazones as PPARγ agonists: Molecular design, synthesis, glucose uptake activity and 3D QSAR studies. *Chem. Cent. J.,* **12**(1): 141.

Mark P. and Nilsson L (2001). Structure and dynamics of the TIP3P, SPC, and SPC/E water models at 298 K. *J. Phys. Chem. A,* **105**(53): 9954-9960.

Mayer K, Eris D, Schwardt O, Sager CP, Rabbani S, Kleeb S and Ernst B (2017). Urinary Tract infection: which conformation of the bacterial lectin fimh is therapeutically relevant? *J. Med. Chem.,* **60**(13): 5646-5662.

Mohammed MA, Alnour TM, Shakurfo OM and Aburass MM (2016). Prevalence and antimicrobial resistance pattern of bacterial strains isolated from patients with urinary tract infection in Messalata Central Hospital, Libya. *Asian Pac. J. Trop. Med.,* **9**(8): 771-776.

Mousavifar L, Touaibia M and Roy R (2018). Development of Mannopyranoside Therapeutics against Adherent-Invasive *Escherichia coli* Infections. *Acc. Chem. Res.,* **51**(11): 2937-2948.

Mousavifar L, Vergoten G, Charron G and Roy R (2019). Comparative study of aryl o-, c- and s-mannopyranosides as potential adhesion inhibitors toward uropathogenic *E. coli* FimH. *Molecules,* **24**(19): 3566.

Mydock-McGrane LK, Cusumano ZT and Janetka JW (2016). Mannose-derived FimH antagonists: A promising anti-virulence therapeutic strategy for urinary tract infections and Crohn's disease. *Expert. Opin. Ther. Pat.,* **26**(2): 175-97.

Mydock-McGrane LK, Hannan TJ and Janetka JW (2017). Rational design strategies for FimH antagonists: new drugs on the horizon for urinary tract infection and Crohn's disease. *Expert Opin. Drug Discov.,* **12**(7): 711-731.

Namjoo A, Sadri SM, Rafeian M, Ashrafi K, Shahin Fard N and Moosavi Azmareh F (2013). Comparing the effects of *Nigella Sativa* extract and gentamicin in treatment of urinary tract infection caused by *E. coli*. *J. Mazandaran Univ. Med. Sci.*, **22**(96): 22-29.

Ofek I, Mirelman D and Sharon N (1977). Adherence of *Escherichia coli* to human mucosal cells mediated by mannose receptors. *Nature,* **265**(5595): 623-625.

Oraiopoulou ME, Tzamali E, Tzedakis G, Liapis E, Zacharakis G, Vakis A, Papamatheakis J and Sakkalis V (2018). Integrating in vitro experiments with *in silico* approaches for Glioblastoma invasion: the role of cell-to-cell adhesion heterogeneity. *Scientific Reports,* **8**(1): 1-13.

Rafsanjany N, Senker J, Brandt S, Dobrindt U and Hensel A (2015). In vivo consumption of cranberry exerts ex vivo antiadhesive activity against fimh-dominated uropathogenic *Escherichia coli*: A combined *in vivo*, *ex vivo* and *in vitro* study of an extract from *Vaccinium macrocarpo*n. *J. Agric. Food Chem.,* **63**(40): 8804-8818.

Ribić R, Meštrović T, Neuberg M and Kozina G (2018). Effective anti-adhesives of uropathogenic *Escherichia coli. Acta. Pharm.,* **68**(1): 1-18.

Rizvi SMD, Shaikh S, Khan M, Biswas D, Hameed N and Shakil S (2014a). Fetzima (levomilnacipran), a drug for major depressive disorder as a dual inhibitor for human serotonin transporters and beta-site amyloid precursor protein cleaving enzyme-1. *CNS Neurol. Disord. Drug Targets,* **13**(8): 1427-31.

Rizvi SMD, Shaikh S, Naaz D, Shakil S, Ahmad A, Haneef M and Abuzenadah AM (2016). Kinetics and molecular docking study of an anti-diabetic drug glimepiride as acetylcholinesterase inhibitor: implication for alzheimer's disease-diabetes dual therapy. *Neurochem. Res.,* **41**(6): 1475-82.

Rizvi SMD, Shakil S, Zeeshan M, Khan MS, Shaikh S, Biswas D, Ahmad A and Kamal MA (2014b). An enzoinformatics study targeting polo-like kinases-1 enzyme: Comparative assessment of anticancer potential of compounds isolated from leaves of *Ageratum houstonianum*. *Pharmacognosy magazine,* **10**(1): 14-21.

Ronald A (2003). The etiology of urinary tract infection: traditional and emerging pathogens. *Dis. Mon.,* **49**: 71-82.

Sarshar M, Behzadi P, Ambrosi C, Zagaglia C, Palamara AT and Scribano D (2020). FimH and anti-adhesive therapeutics: A disarming strategy against uropathogens. *Antibiotics*, **9**(7): 397.

Schwardt O, Rabbani S, Hartmann M, Abgottspon D, Wittwer M, Kleeb S, Zalewski A, Smiesko M, Cutting B and Ernst B (2011). Design, synthesis and biological evaluation of mannosyl triazoles as FimH antagonists. *Bioorg. Med. Chem.,* **19**(21): 6454-6473.

Shaikh S, Rizvi SMD, Anis R and Shakil S (2016a). Prevalence of CTX-M resistance marker and integrons among *Escherichia coli* and *Klebsiella pneumoniae* isolates of clinical origin. *Lett. Appl. Microbiol.,* **62**(5): 419-27.

Shaikh S, MD Rizvi S, Hameed N, Biswas D, Khan M, Shakil S and A Kamal M (2014). Aptiom (eslicarbazepine acetate) as a dual inhibitor of β-secretase and voltage-gated sodium channel: advancement in Alzheimer's disease-epilepsy linkage via an enzoinformatics study. *CNS Neurol. Disord. Drug Targets,* **13**(7): 1258-1262.

Shaikh S, Rizvi SMD, Suhail T, Shakil S, M Abuzenadah A, Anis R, Naaz D, Dallol A, Haneef M, Ahmad A and Choudhary L (2016b). Prediction of anti-diabetic drugs as dual inhibitors against acetylcholinesterase and beta-secretase: A neuroinformatics study. *CNS Neurol. Disord. Drug Targets,* **15**(10): 1216-1221.

Shakil S and Khan AU (2010a). Detection of CTX-M-15-producing and carbapenem-resistant *Acinetobacter baumannii* strains from urine from an Indian Hospital. *J. Chemother.,* **22**(5): 324-327.

Shakil S and Khan AU (2010b). Infected foot ulcers in male and female diabetic patients: A clinico-bioinformative study. *Ann. Clin. Microbiol. Antimicrob.,* **9**(1): 2.

Shakil S and Khan AU (2010c). Interaction of CTX-M-15 enzyme with cefotaxime: A molecular modelling and docking study. *Bioinformation,* **4**: 468-72.

Shi C, Yan C, Sui Y, Sun Y, Guo D, Chen Y, Jin T, Peng X, Ma L and Xia X (2017). Thymoquinone inhibits virulence related traits of *Cronobacter sakazakii* ATCC 29544 and has anti-biofilm formation potential. *Front. Microbiol.,* **8**: 2220.

Snyder JA, Lloyd AL, Lockatell CV, Johnson DE and Mobley HL (2006). Role of phase variation of type 1 fimbriae in a uropathogenic *Escherichia coli* cystitis isolate during urinary tract infection. *Infect. Immun.,* **74**(2): 1387-1393.

Srinivasan K (2018). Cumin (*Cuminum cyminum*) and black cumin (*Nigella sativa*) seeds: traditional uses, chemical constituents, and nutraceutical effects. *Food Quality and Safety,* **2**(1): 1-16.

Stahlhut SG, Tchesnokova V, Struve C, Weissman SJ, Chattopadhyay S, Yakovenko O, Aprikian P, Sokurenko EV and Krogfelt KA (2009). Comparative structure-function analysis of mannose-specific FimH adhesins from *Klebsiella pneumoniae* and *Escherichia coli*. *J. Bacteriol.,* **191**(21): 6592-6601.

Tayh G, Al Laham N, Ben Yahia H, Ben Sallem R, Elottol AE and Ben Slama K (2019). Extended-spectrum β-Lactamases among Enterobacteriaceae isolated from urinary tract infections in Gaza Strip, Palestine. *Biomed. Res. Int.*, https://doi.org/10.1155/2019/4041801.

Utami AT (2018). *Nigella sativa* Linn. and lower urinary tract infection treatment. *J Surg Pathol Diagn,* **1**(1): 101.

Verma A, Rizvi SMD, Shaikh S, Ansari MA, Shakil S, Ghazal F, Siddiqui MH, Haneef M and Rehman A (2014). Compounds isolated from *Ageratum houstonianum* inhibit the activity of matrix metalloproteinases (MMP-2 and MMP-9): An oncoinformatics study. *Pharmacogn. Mag.,* **10**(37): 18-26.

Winkler ML, Papp-Wallace KM, Taracila MA and Bonomo RA (2015). Avibactam and inhibitor-resistant SHV β-lactamases. *Antimicrob. Agents Chemother.*, **59**(7): 3700-3709.

Zhou G, Mo WJ, Sebbel P, Min G, Neubert TA, Glockshuber R, Wu XR, Sun TT and Kong XP (2001). Uroplakin Ia is the urothelial receptor for uropathogenic *Escherichia coli*: Evidence from *in vitro* FimH binding. *J. Cell Sci.,* **114**(22): 4095-4103.

Zoete V, Cuendet MA, Grosdidier A and Michielin O (2011). Swiss Param: A fast force field generation tool for small organic molecules. *J Comput Chem,* **32**(11) 2359-2368.

Zorgani A, Almagatef A, Sufya N, Bashein A and Tubbal A (2017). Detection of CTX-M-15 Among uropathogenic *Escherichia coli* isolated from five major hospitals in Tripoli, Libya. *Oman Med. J.,* **32**(4): 322-327.